

Potent but Stealthy: Rethink Profile Pollution against Sequential Recommendation via Bi-level Constrained Reinforcement Paradigm

Jiajie Su^{1*}, Zihan Nan^{2*}, Yunshan Ma³, Xiaobo Xia^{4,5}, Xiaohua Feng¹,
Weiming Liu⁶, Xiang Chen¹, Xiaolin Zheng^{1†}, Chaochao Chen¹

¹ Zhejiang University, ² Peking University

³ Singapore Management University, ⁴ National University of Singapore

⁵ MoE Key Laboratory of Brain-inspired Intelligent Perception and Cognition,
University of Science and Technology of China

⁶ Tiktok, Bytedance

{sujiajie, fengxiaohua, wasdnsxchen, xlzheng, zjuccc}@zju.edu.cn,

zhnan25@stu.pku.edu.cn, ysma@smu.edu.sg, xbx@nus.edu.sg, lwming95@gmail.com

Abstract

Sequential Recommenders, which exploit dynamic user intents through interaction sequences, is vulnerable to adversarial attacks. While existing attacks primarily rely on data poisoning, they require large-scale user access or fake profiles thus lacking practicality. In this paper, we focus on the Profile Pollution Attack that subtly contaminates partial user interactions to induce targeted mispredictions. Previous PPA methods suffer from two limitations, *i.e.*, i) over-reliance on sequence horizon impact restricts fine-grained perturbations on item transitions, and ii) holistic modifications cause detectable distribution shifts. To address these challenges, we propose a constrained reinforcement driven attack CREAT that synergizes a bi-level optimization framework with multi-reward reinforcement learning to balance adversarial efficacy and stealthiness. We first develop a Pattern Balanced Rewarding Policy, which integrates pattern inversion rewards to invert critical patterns and distribution consistency rewards to minimize detectable shifts via unbalanced co-optimal transport. Then we employ a Constrained Group Relative Reinforcement Learning paradigm, enabling step-wise perturbations through dynamic barrier constraints and group-shared experience replay, achieving targeted pollution with minimal detectability. Extensive experiments demonstrate the effectiveness of CREAT. The implementation code is released at <https://github.com/SSndot/CREAT>.

Introduction

Sequential Recommendation (SR) (Xie et al. 2022; Liu et al. 2023a; Su et al. 2023a) explores user evolving interests to make the next-item prediction. Although SRs are widely regarded as delivering trustworthy results, their sensitivity to sequential patterns renders them vulnerable to adversarial attacks (Nguyen et al. 2024; Du et al. 2024a). Recent research (Wang et al. 2023; Zhang et al. 2024) has mostly focus on

*These authors contributed equally.

†Xiaolin Zheng is the corresponding author.

Copyright © 2026, Association for the Advancement of Artificial Intelligence (www.aaai.org). All rights reserved.

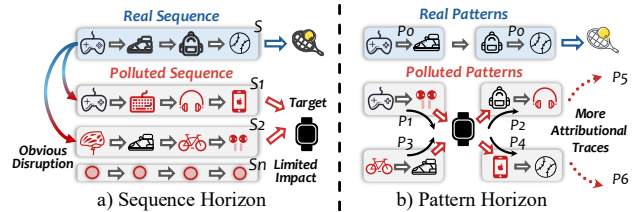


Figure 1: The motivation of CREAT.

data poisoning attacks, which manipulate SR by injecting a substantial amount of crafted sequences. But this attack relies on large-scale access to user accounts or the ability to create numerous fake profiles, which can be impractical in real-world scenarios. In this paper, we focus on a more targeted and stealthier attack strategy, *Profile Pollution Attack (PPA)*, which subtly contaminates partial individual user interaction histories to corrupt SR into a targeted misprediction on specific subtasks.

Several previous studies attempted to conduct PPA against SR. One line of methods (Yue et al. 2021, 2022) crafts perturbations guided by gradient estimation on the attack loss then inserts influential items. Another line (Du et al. 2024b) leverages the influence function to measure the modification impact to training sequences on model parameters. As Fig 1 shows, these works largely follow a common paradigm, *i.e.*, assess the intensity of posterior attacks from the *sequence horizon*, which leverages the global structure of polluted sequences to modify recommender comprehension on user behaviors. Such a paradigm faces two limitations, **(i) Low attack intensity**. Relying on amplification of the whole polluted sequence effect confines the attack to user subsets with specific interests, failing to reshape model perception on fine-grained sequential transitions. **(ii) Subtle attack stealth**. Forcing the overall interests of sequences to align with attack targets induces a noticeable distributional shift. Since interference at the sequence horizon is a coarse-grained and user-level disruption, it often requires manipulating numerous sequences to achieve a significant effect,

thus increasing the detection risk. These issues motivate us to a crucial question: **How to exploit pivotal structures underlying the recommender collaborative modeling to maximize attack strength with minimal detectability?**

In light of this, we reformulate PPA into a bi-level optimization problem, wherein the *upper-level objective* seeks to maximize the utility of sequence perturbations, subject to a *lower-level constraint* enforcing a bounded degree of stealthiness in the crafted sequences. The upper-level formulation is grounded in a new theoretical concept, termed *pattern horizon*, which postulates that the model’s prediction of the next item is inherently driven by an attributional trace over sequential pattern dependencies (Yin et al. 2024; Dang et al. 2025). As Fig 1 shows, inverting pivotal sequential patterns toward a target item enables a finer-grained exploration of how distinct perturbations propagate through the collaborative reasoning process of SR. Due to synergistic and cascading effects between patterns (Liu et al. 2023b), modifying a subset of patterns can be generalized to multiple similar patterns during the SR model’s learning process, thereby amplifying the adversarial impact. At the lower level, in contrast to traditional sequence horizon perturbations that operate on holistic representations, the pattern-horizon-guided perturbations emphasize localized structural shifts. This allows the attacker to strategically calibrate pattern granularity and compositional balance, effectively regulating the distributional deviation between crafted and benign sequences. However, this bi-level formulation raises three key challenges, *i.e.*, **Ch1: How to discern and reverse critical sequential patterns? Ch2: How to modulate the stealthiness of pattern-balanced perturbations? Ch3: How to synergistically optimize the coupled objectives across both levels?**

To tackle these challenges, we propose a Constrained Reinforcement driven ATtack, termed **CREAT**, which leverages a group relative reinforcement learning constrained by stealth-aware conditions for targeted profile pollution. The key insight of **CREAT** lies in simulating the bi-level optimization problem with a multi-reward mechanism, *i.e.*, maximize the inversion effect of critical sequential patterns while minimize detection risk, thereby deriving an optimal pollution policy. For separately regulating the upper-level and lower-level objectives, we design a *Pattern Balanced Rewarding Policy (PBRP)*, integrating both inversion and consistency rewards to guide the perturbation. To uncover the most influential patterns (**Ch1**), we first develop the *pattern inversion reward* which identifies the optimal perturbation positions that simultaneously achieve maximal pattern-level semantic inversion and diversification. To regulate stealthiness of inverted patterns (**Ch2**), the *distribution consistency reward* adapts an unbalanced co-optimal transport to constrain the distributional shifts of polluted sequential representation from both sample and pattern aspects. Building upon the bi-level mechanism, we establish *Constrained Group Relative Reinforcement Learning (C-GRRL)*, which enables step-wise and self-reflective perturbations over polluted sequences. This paradigm consists of two stages, *i.e.*, critical pattern localization and constrained inversion optimization. In the *localization stage*, we train a sequence masker solely guided by the inversion reward, aiming to

identify positions on target items that yield maximal adversarial impact. In the *constrained stage*, a dynamic barrier constraint that adaptively joins inversion and consistency rewards fine-tunes the masker, thereby aligning with the dual imperative of maximizing adversarial efficacy while preserving stealthiness (**Ch3**). Specifically, we employ a constrained group-relative policy within the bi-level optimization, which integrates a group-shared experience replay buffer and relative prioritized sampling, to accelerate the convergence toward optimal multi-step perturbations.

Main contributions are: (1) We revisit the PPA against SR into a bi-level optimization problem, and propose a novel framework with group relative constrained reinforcement learning. (2) We devise the PBRP policy, developing pattern inversion reward to extract influential patterns and distribution consistency reward to control pattern stealth. (3) We establish the C-GRRL paradigm, realizing step-wise and self-reflected perturbation optimization. (4) Extensive experiments demonstrate the effectiveness of **CREAT**.

Related Work

Sequential Recommendation. SR characterizes dynamic user intents by modeling behavioral sequences. Early work models sequential patterns with Markov Chain assumption (Rendle, Freudenthaler, and Schmidt-Thieme 2010). Later, Recurrent Neural Networks (Wu et al. 2017), Convolutional Neural Networks (Tang and Wang 2018), Graph Neural Networks (Wu et al. 2019; Zheng et al. 2020; Su et al. 2023b), and Transformers (Kang and McAuley 2018) are developed to model interests over interactions. Besides, unsupervised learning based models (Xie et al. 2022) extract more informative user patterns by deriving self-supervision signals. Inspired by generative models, a series of diffusion-based SRs (Yang et al. 2023) merge, leveraging diffusion generative capabilities to produce personalized content. A series of methods (Li et al. 2023; Liu et al. 2024b) utilize large language models to enhance the accuracy of SR. But the vulnerability of SR to adversarial attacks based on malicious sequences remains a significant security problem.

Adversarial Attacks in Recommender Systems. Adversarial attacks (Zhang et al. 2021a, 2022; Wang et al. 2023, 2024) on recommender systems can be categorized into: (1) *data poisoning* and (2) *profile pollution*. Data poisoning attacks (Zhang et al. 2020; Song et al. 2020; Tang, Wen, and Wang 2020; Huang et al. 2021; Wu et al. 2023) compromise recommenders by injecting fabricated user profiles, skewing model outputs toward adversarial objectives. Conversely, profile pollution attacks (PPA) (Yue et al. 2021; Zhang et al. 2021b; Fan et al. 2021; Lin et al. 2022) directly tamper with user interaction records, subtly distorting individual recommendation streams without requiring large-scale data infiltration. In this paper, we focus on the PPA and aim to manipulate the recommendation with targeted goals. Existing studies on PPA is divided into four types, which are respectively based on injection (Xing et al. 2013; Meng et al. 2014; Zhang et al. 2019), replacement (Yue et al. 2022), repetition (Tang and Wang 2018), and expert knowledge (Yang, Gong, and Cai 2017). The exploration of PPA against SR re-

mains at a nascent stage. One branch of methods (Yue et al. 2021, 2022) generates perturbations by estimating gradients of attack loss, injecting impactful items into the sequences. SimAlter (Yue et al. 2021) appends adversarial items by extending the targeted fast gradient sign method from the continuous to discrete item space. Replace (Yue et al. 2022) typically utilizes the loss gradient to guide the selection of injected items. However, these gradient-based attacks are constrained by insufficient optimization due to single-step gradient descent (Madry et al. 2017). Another branch of work, like INFAttack (Du et al. 2024b), employs influence function to quantify how modifications affect the model parameters. But the influence computation chain introduces substantial complexity while its accuracy deteriorates with deeper backbones. Although these works promote PPA to some extent, they assess pollution strength from *sequence horizon*, which overlooks exploring fine-grained patterns, thus constraining attack effectiveness and increasing the detection risk.

Methodology

Problem Formulation

Profile Pollution Attack against SR. Let Φ_θ denote a sequential recommender with parameters θ , where users $u \in \mathcal{U}$ and items $v \in \mathcal{V}$ are represented by chronological interaction sequences $\mathbf{s}_u = [v_1, \dots, v_L]$. The recommender is trained on a dataset $\mathcal{D} = \{\mathbf{s}_u \mid u \in \mathcal{U}\}$ with the next-item prediction loss $\mathcal{L}(\cdot)$. The profile pollution attack (PPA) aims to perturb a certain *subset* of training sequences $\mathcal{S} \subseteq \mathcal{D}$ into \mathcal{S}' by replacing limited interactions to maximize the recommendation exposure of a target item $v^* \in \mathcal{V}$. For each polluted sequence, the amount of perturbations M is bound by $M \leq K$, where K is a small constant. We assume the attacker knows the model architecture and loss function, or can obtain a surrogate model through prior extraction. This assumption is justified by recent advances in recommendation model extraction (Yue et al. 2021; Wang et al. 2025; Liu et al. 2025), which demonstrate that black-box recommenders can be reliably approximated with limited or even no user data, resulting in surrogate models with similar hidden representations and output behavior. Formally, the objective of PPA is to construct perturbed sequences as:

$$\hat{\theta} = \arg \min_{\theta} \sum_{\mathbf{s}_u \in (\mathcal{D} \setminus \mathcal{S}) \cup \mathcal{S}'} \mathcal{L}(\mathbf{s}_u; \theta),$$

$$\tilde{\mathcal{S}} = \arg \max_{\mathcal{S}'} \mathbb{E}_{u \sim \mathcal{U}} [\text{ER}(v^* \mid \Phi_{\hat{\theta}}(\mathbf{s}_u))].$$

Here, $\hat{\theta}$ denotes the recommender parameters after pollution and $\tilde{\mathcal{S}}$ indicates the optimal polluted sequences that invert the recommender training to maximize the exposure ratio $\text{ER}(v^* \mid \Phi_{\hat{\theta}}(\mathbf{s}_u))$ of v^* in recommendation lists.

Framework Overview. We present CREAT in Figure 2 and its algorithm in Appendix C. CREAT consists of three components, *i.e.*, *perturbation masker*, *pattern balanced rewarding policy (PBRP)*, and *constrained group relative reinforcement learning (C-GRRL)*. The perturbation masker produces the step-wise masking strategies and is optimized by the

PBRP with bi-level objectives. PBRP develops pattern inversion reward to maximize attack intensity, and distribution consistency reward for stealthy constraints. C-GRRL devises a two-stage optimization to solve the bi-level constrained problem.

Pattern Balanced Rewarding Policy

Perturbation Masker. Given a sequential recommender Φ_θ trained on interaction sequences \mathcal{D} , we design a perturbation masker \mathcal{M}_ψ to identify optimal positions in a subset of training sequences $\mathcal{S} \subseteq \mathcal{D}$ for replacing items with the target item v^* , under a perturbation budget $M \leq K$. Formally, for a sequence $\mathbf{s} = [v_1, \dots, v_L]$, the masker generates a binary mask $\mathbf{m} \in \{0, 1\}^L$ through a *step-wise reinforcement learning process*, where $\mathbf{m}_t = 1$ indicates replacing v_t with v^* . The perturbed sequence is constructed iteratively as:

$$\mathbf{s}^{(i)} = \mathbf{s}^{(i-1)} \odot (1 - \mathbf{m}^{(i)}) + v^* \cdot \mathbf{m}^{(i)},$$

where $\mathbf{m}^{(i)}$ is the mask vector at step i , and \odot denotes element-wise multiplication. Unlike traditional perturbation, our masker follows a pattern balanced rewarding policy. At each step i , the masker selects the next position to perturb based on the current state $\mathbf{s}^{(i-1)}$, and receives the reward based on the adversarial impact of the perturbation.

Pattern Inversion Reward. To amplify the attack effect, we propose a *Pattern Inversion Reward* that guides the masker to identify sub-pattern positions whose semantic distributions are notably different from that of the target item. By inserting the target item adjacent to these semantically divergent sub-patterns, the attacker can construct *spurious attributional paths* that link diverse user intent patterns to the target item. This misleads the recommender into falsely associating varied behavioral cues with the target, thereby increasing its exposure. This reward operates on two complementary dimensions, *i.e.*, the directionality and diversity of inversion pathways. **For the directionality of inversion**, we encourage the masker to maximize the semantic distance between the target item with both historical and future sequential contexts. Let $T^{(i)} = \{t_1, \dots, t_i\}$ denote perturbed positions up to step i . For each $t_j \in T^{(i)}$, we compute embeddings of the predecessor $S_{t_j}^p = \mathbf{s}_{[1:t_j-1]}^{(i)}$ and successor $S_{t_j}^f = \mathbf{s}_{[t_j+1:L]}^{(i)}$ using the representation encoder φ_{rec} of Φ_θ . The directionality reward at step i is:

$$R_{\text{dir}}^{(i)} = \sum_{j=1}^i \left[D\left(\varphi_{\text{rec}}(S_{t_j}^p), \varphi_{\text{rec}}(v^*)\right) + D\left(\varphi_{\text{rec}}(v^*), \varphi_{\text{rec}}(S_{t_j}^f)\right) \right],$$

where $D(\cdot, \cdot)$ is the Euclidean distance. **For the diversity of inversion**, we refine the strategy by leveraging the synergistic effects among attack patterns. This inversion reward is designed to enhance the divergence among attack modes, ensuring heterogeneous attack paths and reduce detection risk. At step i , let $\mathcal{Y}^{(i)}$ be the set of subsequences in $\mathbf{s}^{(i)}$ that exclude target items, we map each subsequence $y_p \in \mathcal{Y}^{(i)}$ to a unit-norm prototype as $\tilde{\varphi}(y_p) = \varphi_{\text{rec}}(y_p) / \|\varphi_{\text{rec}}(y_p)\|$. Then we form the diversity reward with the Gram matrix $G_y^{(i)}$:

$$G_y^{(i)} = [\tilde{\varphi}(y_k)^\top \tilde{\varphi}(y_l)]_{k,l=1}^{|\mathcal{Y}^{(i)}|}, R_{\text{div}}^{(i)} = \log \det \left(G_y^{(i)} \right).$$

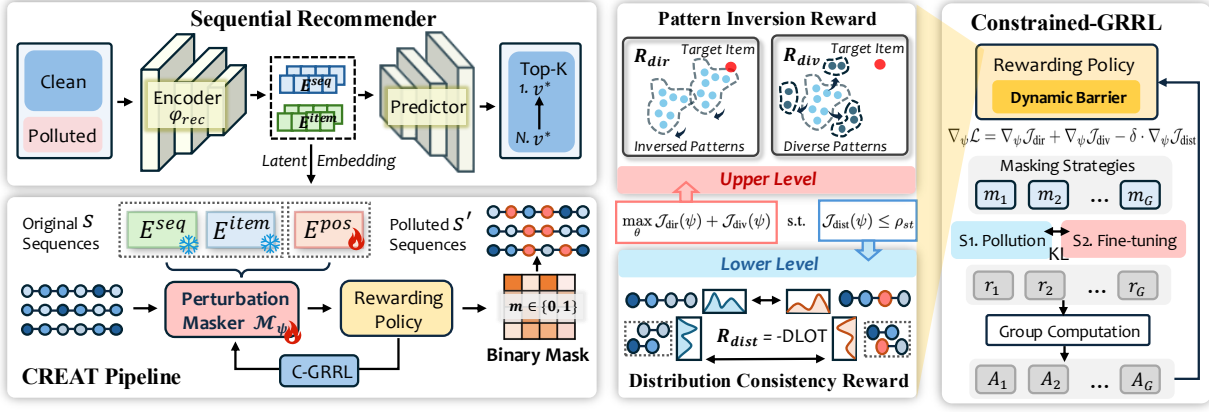


Figure 2: The proposed PPA framework of CREAT, which consists of three components, *i.e.*, the perturbation masker, pattern balanced rewarding policy with inversion and consistency reward, and constrained group relative reinforcement learning.

Distribution Consistency Reward. To ensure the stealthiness of perturbed sequences, we introduce the *Distribution Consistency Reward*, which constrains the deviation between polluted sequences and their original counterparts in both instance-level and pattern-level semantics. We ground this reward in a dual-level co-optimal transport (DLOT) optimization (Tran et al. 2023), which provides a principled measure of distributional shifts by simultaneously aligning global sequence and local transitional patterns. At step i , let s denote the original sequence and $s^{(i)}$ the perturbed sequence. For the sequence-level, we obtain representations from the recommender encoder as $\mathbf{h}_{orig} = \varphi_{rec}(s)$ and $\mathbf{h}_{pert}^{(i)} = \varphi_{rec}(s^{(i)})$. For the pattern-level, the sets $\mathbf{p}_{orig} = \{\varphi_{rec}(s_{[t:t+k]})\}_{t=1}^{L-k}$ and $\mathbf{p}_{pert} = \{\varphi_{rec}(s^{(i)}_{[t:t+k]})\}_{t=1}^{L-k}$ contain k -gram pattern embeddings derived from sliding windows over s and $s^{(i)}$. Then we construct the sequence-pattern spaces from the dual-level representations:

$$\mathbb{X}_{orig} = (\mathbf{h}_{orig}, \mathbf{p}_{orig}, \xi_{orig}), \quad \mathbb{X}_{pert}^{(i)} = (\mathbf{h}_{pert}^{(i)}, \mathbf{p}_{pert}^{(i)}, \xi_{pert}^{(i)}),$$

where ξ_{orig} and ξ_{pert} are scalar functions that define the sample-feature interactions. Unlike traditional balanced OT (Cuturi 2013; Flamary et al. 2021; Liu et al. 2022) and unbalanced OT (Pham et al. 2020; Séjourné, Vialard, and Peyré 2022; Liu et al. 2024c), we incorporate two transport plans in DLOT, *i.e.*, π^s aligns entire sequences while π^f aligns intra-sequence patterns. The optimization of DLOT is:

$$\begin{aligned} DLOT = \inf_{\pi^s, \pi^f} & \iint |\xi_{orig}(\mathbf{h}_{orig}, \mathbf{p}_{orig}) - \xi_{pert}(\mathbf{h}_{pert}^{(i)}, \mathbf{p}_{pert}^{(i)})|^p d\pi^s d\pi^f \\ & + \sum_{j=1}^2 \lambda_j \text{KL}(\pi_{\#j}^s \otimes \pi_{\#j}^f \parallel \mu_j^s \otimes \mu_j^f). \end{aligned}$$

To tolerate partial mass mismatch and enhance robustness, KL-divergence terms penalize deviations of the marginal distributions of π^s and π^f from their empirical counterparts μ^s and μ^f . A mass constraint $m(\pi^s) = m(\pi^f)$ is imposed to ensure transport consistency across levels. We present the derivation details of solving DLOT problem in Appendix A. The consistency reward is set as DLOT distance between as:

$$R_{dist}^{(i)} = -DLOT_{\lambda_1, \lambda_2}(\mathbb{X}_{orig}, \mathbb{X}_{pert}^{(i)}),$$

Constrained Group Relative Learning

To jointly optimize the multi-objective rewards under stealth-aware constraints, we introduce a two-stage optimization paradigm, which enables progressive learning of perturbation strategies by first distilling attack-effective behaviors and then aligning with distributional constraints.

Constrained Reinforcement with Dynamic Barrier. We model the perturbation decision process as a bi-level reinforcement learning problem, where the policy aims to maximize the inversion rewards while satisfying stealth constraints. We formulate the bi-level objective for each mask step, where each reward or constraint term is defined as the expected discounted return:

$$\max_{\theta} \mathcal{J}_{dir}(\psi) + \mathcal{J}_{div}(\psi) \quad \text{s.t.} \quad \mathcal{J}_{dist}(\psi) \leq \rho_{st}$$

$$\mathcal{J}_r(\psi) = \mathbb{E}_{\tau \sim \pi_{\psi}} \left[\sum_{t=0}^T \gamma^t R_r(s_t, a_t, s_{t+1}) \right], \quad r \in \{\text{dir}, \text{div}, \text{dist}\}$$

Here, s_t denotes the state at step t representing the partially perturbed sequence $s^{(i)}$, a_t represents the action of masking, and γ^t is the discount factor. The constraint $\mathcal{J}_{dist}(\psi) \leq \rho_{st}$ enforces stealthiness by bounding the expected distribution consistency reward. It is worth noting that ρ_{st} is a threshold dynamically derived from the distribution of trajectories in group relative policy, which ensures the stealth bound adapts to the evolving policy and group-wise sequence characteristics. To solve this problem, we rewrite the problem as a min-max Lagrangian formulation:

$$\mathcal{L}(\psi, \delta) = \mathcal{J}_{dir}(\psi) + \mathcal{J}_{div}(\psi) - \delta \cdot (\mathcal{J}_{dist}(\psi) - \rho_{st}), \quad \delta \geq 0$$

We compute the policy gradients for each term via the policy gradient theorem, and further derive the policy gradient $\nabla_{\psi} \mathcal{L}$ for perturbation masker \mathcal{M}_{ψ} :

$$\nabla_{\psi} \mathcal{L} = \nabla_{\psi} \mathcal{J}_{dir} + \nabla_{\psi} \mathcal{J}_{div} - \delta \cdot \nabla_{\psi} \mathcal{J}_{dist}.$$

Different from static constraints, we tend to dynamically adjust the penalty term, based on real-time constraint violation and gradient alignment to ensure a balanced optimization. When gradients of $\mathcal{J}_{dir/div}$ and \mathcal{J}_{dist} conflict, the numerator δ reduces to prioritize attack efficacy. Severe stealth

violations increase δ to suppress detectable perturbations. Based on the dynamic barrier design (Gong and Liu 2021), we can give out the closed-form expression as

$$\delta = \left[\frac{\mathcal{J}_{\text{dist}} - \rho_{st} - \nabla_{\psi} \mathcal{J}_{\text{dist}}^{\top} \nabla_{\psi} (\mathcal{J}_{\text{dir}} + \mathcal{J}_{\text{div}})}{\|\nabla_{\psi} \mathcal{J}_{\text{dist}}\|^2 + \kappa} \right]_{+}$$

$\kappa > 0$ is for numerical stability. Then policy gradients are

$$\begin{aligned} \nabla_{\psi} (\mathcal{J}_{\text{dir}} + \mathcal{J}_{\text{div}}) &= \mathbb{E}_{\tau} \left[\sum_t \nabla_{\psi} \log \pi_{\psi}(a_t | s_t) \cdot (\hat{A}_{R_{\text{dir}}} + \hat{A}_{R_{\text{div}}}) \right], \\ \nabla_{\psi} \mathcal{J}_{\text{dist}} &= \mathbb{E}_{\tau} \left[\sum_t \nabla_{\psi} \log \pi_{\psi}(a_t | s_t) \cdot \hat{A}_{R_{\text{dist}}}(s_t, a_t) \right]. \end{aligned}$$

This ensures the policy prioritizes stealthiness only when constraints are violated, balancing efficacy and detectability without sacrificing convergence stability. The perturbation policy is updated using gradient ascent on the Lagrangian as $\psi_{t+1} = \psi_t + \eta (\nabla_{\psi} \mathcal{J}_{\text{dir}} + \nabla_{\psi} \mathcal{J}_{\text{div}} - \delta \cdot \nabla_{\psi} \mathcal{J}_{\text{dist}})$, where η denotes the learning rate. Detailed derivations of this part are in Appendix B.

Group Relative Optimization. To stabilize optimization and accelerate convergence, inspired by the GRPO paradigm (Liu et al. 2024a), we further reform the constrained reinforcement learning with a group relative strategy. Formally, we divide the training into two stages, i.e., *localization stage* and *constrained fine-tuning stage*. In the localization stage, we train the perturbation masker using only the pattern-level rewards R_{dir} and R_{div} . This stage is analogous to supervised fine-tuning, allowing the policy to explore effective inversion behaviors in an unconstrained space. We obtain the masker policy with the pure attacking goal as π_{att} . In the constrained stage, we introduce the distribution consistency reward R_{dist} as a constraint and perform constrained reinforcement learning with dynamic barrier, guided by a GRPO-based surrogate objective. In each masking step, we sample a group of G trajectories $\{o_{i,t}, r_{i,t}\}_{i=1}^G$ under the current policy π_{ψ} , where $o_{i,t}$ is the trajectory and $r_{i,t}$ is the reward aggregated from multi-objective signals. We obtain the group-wise baseline $\mu_{G,t} = \frac{1}{G} \sum_{i=1}^G r_{i,t}$ and reward standard deviation $\sigma_{G,t} = \sqrt{\frac{1}{G-1} \sum_{i=1}^G (r_{i,t} - \mu_{G,t})^2}$. Besides, we can also set the dynamic stealthy threshold for the constraint reward as $\rho_{st} = \mu_G^{\text{dist}} + \lambda_{st} \cdot \sigma_G^{\text{dist}}$. We construct the normalized advantage estimate $\hat{A}_{i,t} = \frac{r_{i,t} - \mu_{G,t}}{\sigma_{G,t} + \epsilon}$, where ϵ is a positive constant for numerical stability. Finally, the policy is optimized with a clipped surrogate objective:

$$\begin{aligned} \mathcal{J}(\psi) &= \mathbb{E}_{\tau} \left[\frac{1}{G} \sum_{i=1}^G \frac{1}{\|o_i\|} \sum_{t=1}^{\|o_i\|} \min \left(\frac{\pi_{\psi}(o_{i,t})}{\pi_{\text{att}}(o_{i,t})} \hat{A}_{i,t}, \right. \right. \\ &\quad \left. \left. \text{clip} \left(\frac{\pi_{\psi}(o_{i,t})}{\pi_{\text{att}}(o_{i,t})}, 1 - \epsilon, 1 + \epsilon \right) \hat{A}_{i,t} \right) \right] \end{aligned}$$

This group relative normalization enhances training stability by reducing sensitivity to outliers and scales advantage estimates adaptively across trajectories. Combining this with bi-level optimization, C-GRRL supports efficient and stable learning of stealthy, high-impact perturbation strategies.

Empirical Study

Experimental Setups

Datasets. Following (Yue et al. 2022), we evaluate on three datasets, i.e. ML-1M, ML-20M, and Amazon Beauty, and preprocess them according to (Sun et al. 2019). The last two items in each sequence are reserved for validation and testing, with the rest assigned to training. The details of datasets are shown in Appendix D.

Backbone Recommender Systems. We choose two representative SR: 1) **NARM** (Li et al. 2017) integrates a GRU-based global and local encoder for sequential modeling. 2) **BERT4Rec** (Sun et al. 2019) employs a transformer-based architecture with bidirectional self-attention.

Comparison Methods. For fair comparison, we set all attack SOTAs under the same setting, i.e., PPA against white-box SR: 1) **Popular Attack** injects sequences with target items and filler popular items. 2) **Random Attack** is similar to the popular attack, but randomly selects filler items. 3) **SimAlter Attack** (Yue et al. 2021) constructs adversarial sequences with semantic associations by calculating the gradient perturbation direction. 4) **Replace Attack** (Yue et al. 2022) identifies fragile items by the sequence gradient information and replaces them with adversarial candidates. 5) **SSL Attack** (Wang et al. 2023) realizes data poisoning against SR with generative adversarial networks, and we adapt it into our white-box setting for fair comparison.

Evaluation Protocols. We evaluate with the exposure ratio of the target item, which is measured with Hit Ratio (HR), Normalized Discounted Cumulative Gain (NDCG), and Mean Reciprocal Rank (MRR). We set the cut-off of the ranked list as 1, 5, and 10. For all the experiments, we repeat them five times and report the average results. The statistical significance tests are conducted by performing t -tests.

Implementation Details. We present the implementation details and parameter settings in Appendix D.

Experimental Results and Analysis

Overall Attack Performance (RQ1). We evaluate the attack performance of CREAT and baselines on NARM and Bert4Rec for three datasets. From Table 1, we find: 1) CREAT significantly enhances target item exposure across diverse scenarios, delivering nearly ten times higher exposure compared to *Pure*. Specifically, it outperforms the best baselines by over 20% across all metrics. 2) Dense datasets favor appending strategies (e.g., Random, Popular), whereas short sequences exhibit heightened susceptibility to substitution strategies (e.g., SimAlter, Replace). The divergence emerges as longer sequences intensify positional bias in attention mechanisms, while shorter sequences' dependence on sparse high-impact features elevates substitution risks. 3) On the most challenging dataset, i.e., *Beauty*, all baselines exhibit poor attack performance, e.g., the well-performed SOTA *SSL Attack* only achieve 0.0109 on HR@10. In contrast, CREAT achieved 0.2601 on HR@10 and 0.1038 on NDCG@10, highlighting the superior efficacy of deep pattern extraction over gradient-based strategies.

Attack	NARM						Bert4Rec					
	HR@1	HR@5	HR@10	NDCG@5	NDCG@10	MRR	HR@1	HR@5	HR@10	NDCG@5	NDCG@10	MRR
ML-1M												
Pure	0.0038	0.0109	0.0174	0.0075	0.0096	0.0098	0.0000	0.0076	0.0128	0.0034	0.0051	0.0062
Popular	0.0128	0.0428	0.0695	0.0280	0.0365	0.0406	0.0105	<u>0.0632</u>	<u>0.1065</u>	<u>0.0372</u>	<u>0.0515</u>	0.0452
Random	0.0104	0.0326	0.0560	0.0217	0.0291	0.0333	0.0043	0.0305	0.0560	0.0173	0.0255	0.0254
SimAlter	0.0143	0.0459	0.0658	0.0306	0.0369	0.0360	0.0102	0.0385	0.0563	0.0271	0.0328	0.0324
Replace	<u>0.0164</u>	<u>0.0575</u>	0.1027	<u>0.0369</u>	<u>0.0515</u>	0.0514	<u>0.0155</u>	0.0569	0.0938	0.0365	0.0493	<u>0.0512</u>
SSLAttack	0.0148	0.0565	<u>0.1069</u>	0.0350	0.0510	<u>0.0564</u>	0.0145	0.0578	0.0970	0.0356	0.0483	0.0453
CREAT	0.0305	0.0855	0.1428	0.0580	0.0765	0.0749	0.0187	0.0811	0.1492	0.0448	0.0666	0.0593
Beauty												
Pure	0.0003	0.0015	0.0033	0.0008	0.0014	0.0021	0.0000	0.0000	0.0000	0.0000	0.0000	0.0022
Popular	0.0005	0.0018	0.0065	0.0009	0.0023	0.0032	0.0000	0.0000	0.0000	0.0000	0.0000	0.0026
Random	0.0010	0.0051	0.0103	0.0029	0.0042	0.0049	0.0000	0.0000	0.0001	0.0000	0.0000	0.0031
SimAlter	0.0019	0.0093	0.0178	0.0055	0.0082	0.0116	0.0000	0.0013	0.0048	0.0006	0.0017	0.0068
Replace	0.0027	0.0151	0.0608	0.0070	0.0216	0.0228	0.0000	0.0000	0.0000	0.0000	0.0000	0.0034
SSLAttack	0.0095	0.0354	0.0751	0.0226	0.0296	0.0270	0.0022	0.0074	0.0109	0.0049	0.0060	0.0097
CREAT	0.0424	0.1080	0.1504	0.0759	0.0895	0.0801	0.0076	0.1191	0.2601	0.0582	0.1038	0.0773
ML-20M												
Pure	0.0020	0.0108	0.0215	0.0063	0.0097	0.0136	0.0001	0.0015	0.0046	0.0007	0.0018	0.0070
Popular	<u>0.0516</u>	<u>0.1516</u>	<u>0.2207</u>	<u>0.1024</u>	<u>0.1247</u>	<u>0.1074</u>	0.0201	<u>0.1542</u>	<u>0.2431</u>	<u>0.0905</u>	<u>0.1171</u>	<u>0.0945</u>
Random	0.0411	0.1287	0.2080	0.0851	0.1096	0.1019	0.0193	0.1062	0.1634	0.0746	0.0930	0.0892
SimAlter	0.0318	0.1204	0.2048	0.0756	0.1036	0.0955	<u>0.0235</u>	0.0815	0.1398	0.0523	0.0710	0.0662
Replace	0.0356	0.1243	0.1906	0.0799	0.1012	0.0921	0.0084	0.0455	0.0872	0.0269	0.0402	0.0420
SSLAttack	0.0437	0.1202	0.1743	0.0825	0.0999	0.0893	0.0217	0.0723	0.1135	0.0473	0.0605	0.0583
CREAT	0.0585	0.1905	0.3041	0.1243	0.1608	0.1392	0.0241	0.1621	0.2628	0.0932	0.1255	0.1025

Table 1: The overall performance on three datasets. The best results are boldfaced, and the second-best results are underlined. All improvements are significant with p -value < 0.05 based on t -tests.

Attack	NARM				Bert4Rec			
	ML-1M		Beauty		ML-1M		Beauty	
	H@10	N@10	H@10	N@10	H@10	N@10	H@10	N@10
w/o dir	0.0117	0.0024	0.5105	0.3663	0.0140	0.0056	0.6307	0.4812
w/o div	0.0143	0.0055	0.5547	0.4318	0.0151	0.0063	0.6603	0.5941
w/o pv	0.0025	0.0013	0.5051	0.3538	0.0053	0.0019	0.5044	0.2859
w/o dist	0.0271	0.0116	0.6291	0.5221	0.0212	0.0083	0.7461	0.7034
CREAT	0.0157	0.0063	0.5633	0.4439	0.0186	0.0068	0.6885	0.6285

Table 2: Ablation studies on each reward.

Ablation Studies (RQ2). To evaluate impact of each reward in policy, we design variants as: (a) *w/o dir* removes the directionality reward. (b) *w/o div* removes the diversity reward. (c) *w/o pv* removes the whole pattern inversion reward. (d) *w/o dist* removes the distribution consistency reward. From Table 2, we conclude: 1) *w/o dir* and *w/o div* both outperform *w/o pv*, showing that either the directionality or diversity reward contributes to the promotion. 2) CREAT performs better than *w/o dir* and *w/o div*, showing that relying solely on either pattern reward has its limitations. Utilizing only R_{dir} leads to the clustering of inverted patterns in the representation space, while solely on R_{div} results in insufficient disturbance of the sub-patterns. 3) The constrained reward R_{dist} decreases attack effectiveness on both datasets, but its impact varies. This is due to different behavioral characteristics, *i.e.*, high randomness in user behavior makes patterns more fragile, while stable preferences allow effective feature injection even under covert conditions.

Stealth Verification (RQ3). We evaluate the stealthiness of CREAT from three aspects. *First*, we present the performance of each attack under the defense SOTA methods in Appendix E, where we prove CREAT still outperforms other attacks even under the strongest defenses. *Second*, we

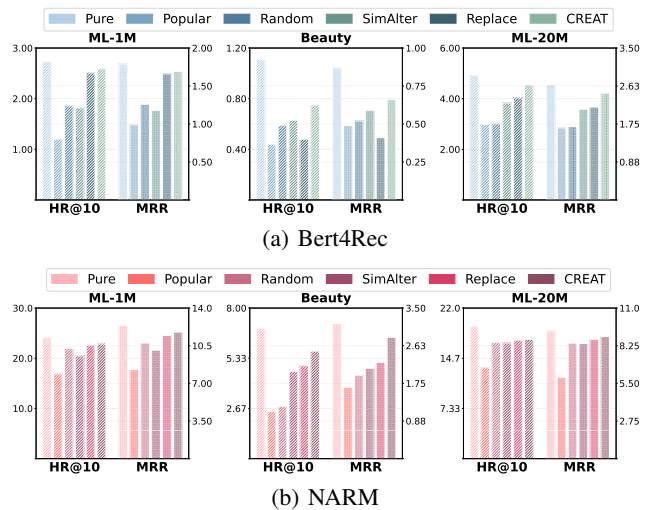


Figure 3: Effects on recommendation accuracy (%).

evaluate the side effects that each PPA brings to the overall SR performance. We present the recommendation accuracy of all users on both backbones before and after PPA in Figure 3. From it, we observe all attacks damage the performance of SR. Compared to SOTAs, CREAT results in slighter accuracy degradation across all datasets, indicating that: 1) CREAT efficiently attacks by uncovering finer-grained sequential pattern correlations with minimal disturbance. 2) Since CREAT causes less degradation in the overall accuracy, it is less likely to trigger detection mechanisms that rely on fluctuations in SR performance, thereby making the attack more stealthy. *Third*, we employ t-SNE (Van der Maaten and Hinton 2008) to visualize the latent distribution

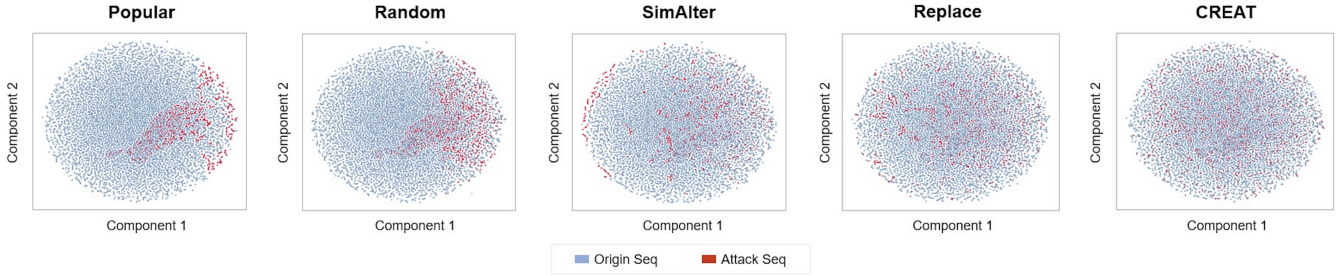


Figure 4: The t-SNE visualization of original sequences and polluted sequences.

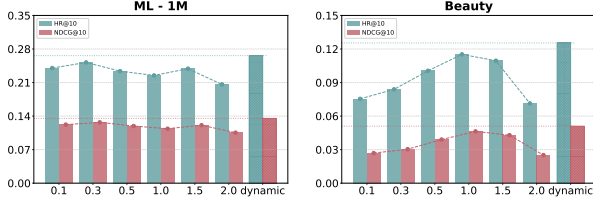


Figure 5: The effects of the dynamic barrier.

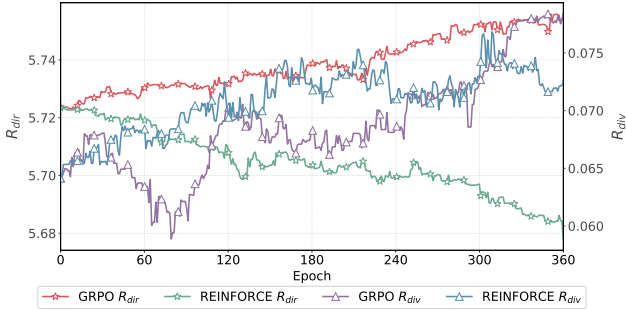


Figure 6: The convergence of CREAT.

of original sequences and polluted sequences. From Figure 4, we find: 1) the adversarial samples from *Popular* and *Random* are distinguishable from original samples, while *SimAlter* with feature alignment improves stealth but still has detectable anomalies. 2) Compared to the best SOTA *Replace*, CREAT shows further enhancement in stealth, achieving indistinguishability between polluted and clean sequences, indicating high integration in spatial density, local clustering patterns, and edge distribution features.

Adaptability of Dynamic Barrier (RQ4). To justify necessity of dynamically adjusting constraint penalty, we replace the constrained reinforcement with *dynamic barrier* by fixed penalty coefficients. From Figure 5, we observe that setting the penalty to static values, *i.e.*, ranging from 0.1 to 2.0, leads to suboptimal or unstable performance. Contrastingly, CREAT achieves the best performance, indicating the ability of dynamic barrier to adaptively adjust the penalty in response to constraint violations and optimization dynamics.

GRPO Convergence (RQ5). We prove GRPO’s convergence through first-360-epoch reward trajectories, compared with traditional REINFORCE. Figure 6 shows REINFORCE preserves consistency reward but suffers persistent pattern inversion reward decline due to its lack of group-wise baseline normalization for reward functions, whereas GRPO achieves sustained pattern inversion reward growth stabilizing post-epoch-300. Despite initial volatility,

Attack	NARM			Bert4Rec		
	Head	Medium	Tail	Head	Medium	Tail
ML-1M						
Pure	0.0513	0.0174	0.0000	0.2149	0.0128	0.0000
SimAlter	0.3079	0.0658	0.0000	0.3081	0.0563	0.0000
Replace	0.3535	0.1027	0.0036	0.4829	0.0938	0.0000
CREAT	0.5664	0.1428	0.0451	0.5228	0.1492	0.0707
Beauty						
Pure	0.0472	0.0033	0.0000	0.0254	0.0000	0.0000
SimAlter	0.1504	0.0178	0.0004	0.5277	0.0048	0.0000
Replace	0.3350	0.0608	0.0000	0.4947	0.0000	0.0000
CREAT	0.4714	0.1504	0.0102	0.6587	0.2601	0.1999
ML-20M						
Pure	0.0974	0.0215	0.0000	0.2139	0.0046	0.0000
SimAlter	0.4031	0.2048	0.0000	0.3401	0.1398	0.0000
Replace	0.3865	0.1906	0.0000	0.3816	0.0872	0.0000
CREAT	0.4317	0.3041	0.0953	0.4590	0.2628	0.1502

Table 3: Attack across various target popularity (HR@10).

GRPO’s consistency reward stabilizes post-epoch-120 and converges post-epoch-330, confirming its capability.

Effect of Target Item Popularity (RQ6). To investigate the effect of target item popularity on attacks, we conduct more experiments. From Table 3, we find: 1) *SimAlter* and *Replace* exhibit significantly weaker tail-item attack capabilities than CREAT, demonstrating near-zero efficacy across all datasets. 2) CREAT exhibits superior exposures across all range of popularity. Our attack demonstrates a greater relative improvement on lower-popularity targets, with tail items exhibit higher enhancement than medium and head targets. Since attackers in real scenarios typically focus on increasing the illicit exposure of long-tail items rather than already popular ones, this advantage has practical significance.

Conclusion and Future Work

We rethink the PPA against SR into a bi-level optimization problem with upper-level objective as attack intensity and lower-level as attack stealthiness. In the proposed CREAT, we first design a pattern balanced rewarding policy to reverse key patterns and reduce observable deviations. Then we implement a constrained group relative reinforcement learning, leveraging dynamic constraints and group-shared experience replay. Extensive experiments demonstrate the effectiveness and stealth of CREAT. CREAT exhibit superior attack effectiveness, but there are currently no effective defenses against such attacks, which pose potential security risks to recommenders. In the future, we will extend adaptive defenses against such attacks for recommender safety.

Acknowledgments

This work is supported by the National Natural Science Foundation of China (Grant No.72192823 and No.624B2131) and the Fundamental Research Funds for the Central Universities. Xiaobo Xia is partially supported by the MoE Key Laboratory of Brain-inspired Intelligent Perception and Cognition at the University of Science and Technology of China (Grant No. 2421002).

References

- Cuturi, M. 2013. Sinkhorn distances: Lightspeed computation of optimal transport. *Advances in neural information processing systems*, 26.
- Dang, Y.; Liu, Y.; Yang, E.; Huang, M.; Guo, G.; Zhao, J.; and Wang, X. 2025. Data augmentation as free lunch: Exploring the test-time augmentation for sequential recommendation. In *Proceedings of the 48th International ACM SIGIR Conference on Research and Development in Information Retrieval*, 1466–1475.
- Du, L.; Yuan, Q.; Chen, M.; Sun, M.; Cheng, P.; Chen, J.; and Zhang, Z. 2024a. PARL: Poisoning Attacks Against Reinforcement Learning-based Recommender Systems. In *Proceedings of the 19th ACM Asia Conference on Computer and Communications Security*, 1331–1344.
- Du, X.; Chen, Y.; Zhang, Y.; and Tang, J. 2024b. Precision Profile Pollution Attack on Sequential Recommenders via Influence Function. *arXiv preprint arXiv:2412.01127*.
- Fan, W.; Derr, T.; Zhao, X.; Ma, Y.; Liu, H.; Wang, J.; Tang, J.; and Li, Q. 2021. Attacking black-box recommendations via copying cross-domain user profiles. In *2021 IEEE 37th international conference on data engineering (ICDE)*, 1583–1594. IEEE.
- Flamary, R.; Courty, N.; Gramfort, A.; Alaya, M. Z.; Boissunon, A.; Chambon, S.; Chapel, L.; Corenflos, A.; Fatras, K.; Fournier, N.; et al. 2021. Pot: Python optimal transport. *Journal of Machine Learning Research*, 22(78): 1–8.
- Gong, C.; and Liu, X. 2021. Bi-objective trade-off with dynamic barrier gradient descent. *NeurIPS 2021*.
- Huang, H.; Mu, J.; Gong, N. Z.; Li, Q.; Liu, B.; and Xu, M. 2021. Data poisoning attacks to deep learning based recommender systems. *arXiv preprint arXiv:2101.02644*.
- Kang, W.-C.; and McAuley, J. 2018. Self-attentive sequential recommendation. In *ICDM*, 197–206. IEEE.
- Li, J.; Ren, P.; Chen, Z.; Ren, Z.; Lian, T.; and Ma, J. 2017. Neural attentive session-based recommendation. In *Proceedings of the 2017 ACM on Conference on Information and Knowledge Management*, 1419–1428.
- Li, J.; Zhang, W.; Wang, T.; Xiong, G.; Lu, A.; and Medioni, G. 2023. GPT4Rec: A generative framework for personalized recommendation and user interests interpretation. *arXiv preprint arXiv:2304.03879*.
- Lin, C.; Chen, S.; Zeng, M.; Zhang, S.; Gao, M.; and Li, H. 2022. Shilling black-box recommender systems by learning to generate fake user profiles. *IEEE Transactions on Neural Networks and Learning Systems*, 35(1): 1305–1319.
- Liu, A.; Feng, B.; Xue, B.; Wang, B.; Wu, B.; Lu, C.; Zhao, C.; Deng, C.; Zhang, C.; Ruan, C.; et al. 2024a. Deepseek-v3 technical report. *arXiv preprint arXiv:2412.19437*.
- Liu, F.; Zhang, H.; Lan, Y.; and Li, M. 2025. FewMEA: Few-shot Model Extraction Attack against Sequential Recommenders. In *Proceedings of the 2025 International Conference on Multimedia Retrieval, ICMR '25*, 917–925. New York, NY, USA: Association for Computing Machinery. ISBN 9798400718779.
- Liu, Q.; Wu, X.; Wang, Y.; Zhang, Z.; Tian, F.; Zheng, Y.; and Zhao, X. 2024b. Llm-esr: Large language models enhancement for long-tailed sequential recommendation. In *NeurIPS*, volume 37, 26701–26727.
- Liu, W.; Chen, C.; Liao, X.; Hu, M.; Su, J.; Tan, Y.; and Wang, F. 2024c. User distribution mapping modelling with collaborative filtering for cross domain recommendation. In *Proceedings of the ACM Web Conference 2024*, 334–343.
- Liu, W.; Zheng, X.; Chen, C.; Su, J.; Liao, X.; Hu, M.; and Tan, Y. 2023a. Joint internal multi-interest exploration and external domain alignment for cross domain sequential recommendation. In *Proceedings of the ACM Web Conference 2023*, 383–394.
- Liu, W.; Zheng, X.; Su, J.; Hu, M.; Tan, Y.; and Chen, C. 2022. Exploiting Variational Domain-Invariant User Embedding for Partially Overlapped Cross Domain Recommendation. In *The 45th International ACM SIGIR Conference on Research and Development in Information Retrieval, Madrid, Spain, July 11 - 15, 2022*, 312–321. ACM.
- Liu, X.; Li, Z.; Gao, Y.; Yang, J.; Cao, T.; Wang, Z.; Yin, B.; and Song, Y. 2023b. Enhancing user intent capture in session-based recommendation with attribute patterns. *Advances in Neural Information Processing Systems*, 36: 30821–30839.
- Madry, A.; Makelov, A.; Schmidt, L.; Tsipras, D.; and Vladu, A. 2017. Towards deep learning models resistant to adversarial attacks. *arXiv preprint arXiv:1706.06083*.
- Meng, W.; Xing, X.; Sheth, A.; Weinsberg, U.; and Lee, W. 2014. Your online interests: Pwned! a pollution attack against targeted advertising. In *Proceedings of the 2014 ACM SIGSAC Conference on Computer and Communications Security*, 129–140.
- Nguyen, T. T.; Quoc Viet hung, N.; Nguyen, T. T.; Huynh, T. T.; Nguyen, T. T.; Weidlich, M.; and Yin, H. 2024. Manipulating Recommender Systems: A Survey of Poisoning Attacks and Countermeasures. *ACM Computing Surveys*, 57(1).
- Pham, K.; Le, K.; Ho, N.; Pham, T.; and Bui, H. 2020. On unbalanced optimal transport: An analysis of sinkhorn algorithm. In *International Conference on Machine Learning*, 7673–7682. PMLR.
- Rendle, S.; Freudenthaler, C.; and Schmidt-Thieme, L. 2010. Factorizing personalized markov chains for next-basket recommendation. In *WWW*, 811–820.
- Séjourné, T.; Vialard, F.-X.; and Peyré, G. 2022. Faster unbalanced optimal transport: Translation invariant sinkhorn and 1-d frank-wolfe. In *International Conference on Artificial Intelligence and Statistics*, 4995–5021. PMLR.

- Song, J.; Li, Z.; Hu, Z.; Wu, Y.; Li, Z.; Li, J.; and Gao, J. 2020. Poisonrec: an adaptive data poisoning framework for attacking black-box recommender systems. In *2020 IEEE 36th international conference on data engineering (ICDE)*, 157–168. IEEE.
- Su, J.; Chen, C.; Lin, Z.; Li, X.; Liu, W.; and Zheng, X. 2023a. Personalized Behavior-Aware Transformer for Multi-Behavior Sequential Recommendation. In *Proceedings of the 31st ACM International Conference on Multimedia, MM '23*, 6321–6331. New York, NY, USA: Association for Computing Machinery. ISBN 9798400701085.
- Su, J.; Chen, C.; Liu, W.; Wu, F.; Zheng, X.; and Lyu, H. 2023b. Enhancing hierarchy-aware graph networks with deep dual clustering for session-based recommendation. In *Proceedings of the ACM web conference 2023*, 165–176.
- Sun, F.; Liu, J.; Wu, J.; Pei, C.; Lin, X.; Ou, W.; and Jiang, P. 2019. BERT4Rec: Sequential Recommendation with Bidirectional Encoder Representations from Transformer. arXiv:1904.06690.
- Tang, J.; and Wang, K. 2018. Personalized top-n sequential recommendation via convolutional sequence embedding. In *WSDM*, 565–573.
- Tang, J.; Wen, H.; and Wang, K. 2020. Revisiting adversarially learned injection attacks against recommender systems. In *Proceedings of the 14th ACM Conference on Recommender Systems*, 318–327.
- Tran, Q. H.; Janati, H.; Courty, N.; Flamary, R.; Redko, I.; Demetci, P.; and Singh, R. 2023. Unbalanced co-optimal transport. In *Proceedings of the AAAI Conference on Artificial Intelligence*, volume 37, 10006–10016.
- Van der Maaten, L.; and Hinton, G. 2008. Visualizing data using t-SNE. *Journal of machine learning research*, 9(11).
- Wang, Y.; Su, J.; Chen, C.; Han, M.; Zhang, C.; and Wang, J. 2025. Sim4Rec: Data-Free Model Extraction Attack on Sequential Recommendation. *Proceedings of the AAAI Conference on Artificial Intelligence*, 39(12): 12766–12774.
- Wang, Z.; Gao, M.; Yu, J.; Ma, H.; Yin, H.; and Sadiq, S. 2024. Poisoning attacks against recommender systems: A survey. *arXiv preprint arXiv:2401.01527*.
- Wang, Z.; Yu, J.; Gao, M.; Yin, H.; Cui, B.; and Sadiq, S. 2023. Poisoning Attacks Against Contrastive Recommender Systems. *arXiv preprint arXiv:2311.18244*.
- Wu, C.; Lian, D.; Ge, Y.; Zhu, Z.; and Chen, E. 2023. Influence-driven data poisoning for robust recommender systems. *IEEE Transactions on Pattern Analysis and Machine Intelligence*, 45(10): 11915–11931.
- Wu, C.-Y.; Ahmed, A.; Beutel, A.; Smola, A. J.; and Jing, H. 2017. Recurrent recommender networks. In *WSDM*, 495–503.
- Wu, S.; Tang, Y.; Zhu, Y.; Wang, L.; Xie, X.; and Tan, T. 2019. Session-based recommendation with graph neural networks. In *AAAI*, volume 33, 346–353.
- Xie, X.; Sun, F.; Liu, Z.; Wu, S.; Gao, J.; Zhang, J.; Ding, B.; and Cui, B. 2022. Contrastive learning for sequential recommendation. In *ICDE*, 1259–1273. IEEE.
- Xing, X.; Meng, W.; Doozan, D.; Snoeren, A. C.; Feamster, N.; and Lee, W. 2013. Take this personally: Pollution attacks on personalized services. In *22nd USENIX Security Symposium (USENIX Security 13)*, 671–686.
- Yang, G.; Gong, N. Z.; and Cai, Y. 2017. Fake co-visitation injection attacks to recommender systems. In *NDSS*.
- Yang, Z.; Wu, J.; Wang, Z.; Wang, X.; Yuan, Y.; and He, X. 2023. Generate what you prefer: Reshaping sequential recommendation via guided diffusion. In *NeurIPS*, 24247–24261.
- Yin, M.; Wang, H.; Guo, W.; Liu, Y.; Zhang, S.; Zhao, S.; Lian, D.; and Chen, E. 2024. Dataset regeneration for sequential recommendation. In *Proceedings of the 30th ACM SIGKDD Conference on Knowledge Discovery and Data Mining*, 3954–3965.
- Yue, Z.; He, Z.; Zeng, H.; and McAuley, J. 2021. Black-box attacks on sequential recommenders via data-free model extraction. In *RecSys*, 44–54.
- Yue, Z.; Zeng, H.; Kou, Z.; Shang, L.; and Wang, D. 2022. Defending substitution-based profile pollution attacks on sequential recommenders. In *RecSys*, 59–70.
- Zhang, H.; Li, Y.; Ding, B.; and Gao, J. 2020. Practical data poisoning attack against next-item recommendation. In *WWW*, 2458–2464.
- Zhang, H.; Tian, C.; Li, Y.; Su, L.; Yang, N.; Zhao, W. X.; and Gao, J. 2021a. Data poisoning attack against recommender system using incomplete and perturbed data. In *Proceedings of the 27th ACM SIGKDD Conference on Knowledge Discovery & Data Mining*, 2154–2164.
- Zhang, K.; Cao, Q.; Wu, Y.; Sun, F.; Shen, H.; and Cheng, X. 2024. Lorec: Large language model for robust sequential recommendation against poisoning attacks. *arXiv preprint arXiv:2401.17723*.
- Zhang, S.; Yin, H.; Chen, T.; Huang, Z.; Nguyen, Q. V. H.; and Cui, L. 2022. Pipattack: Poisoning federated recommender systems for manipulating item promotion. In *Proceedings of the Fifteenth ACM International Conference on Web Search and Data Mining*, 1415–1423.
- Zhang, X.; Chen, J.; Zhang, R.; Wang, C.; and Liu, L. 2021b. Attacking recommender systems with plausible profile. *IEEE Transactions on Information Forensics and Security*, 16: 4788–4800.
- Zhang, Y.; Xiao, J.; Hao, S.; Wang, H.; Zhu, S.; and Jajodia, S. 2019. Understanding the manipulation on recommender systems through web injection. *IEEE Transactions on Information Forensics and Security*, 15: 3807–3818.
- Zheng, Y.; Liu, S.; Li, Z.; and Wu, S. 2020. Dgtn: Dual-channel graph transition network for session-based recommendation. In *ICDMW*, 236–242. IEEE.

Appendix

A Distribution Consistency Reward

This section presents the complete formulation and optimization procedure for the Dual-Level co-Optimal Transport (DLOT) reward, which we use to quantify semantic consistency between the original and perturbed sequences.

DLOT Formulation

Let \mathbf{s} denote the original user sequence and $\mathbf{s}^{(i)}$ its perturbed counterpart. Their corresponding global sequence embeddings from the recommender encoder are:

$$\mathbf{h}_{\text{orig}} = \varphi_{\text{rec}}(\mathbf{s}), \quad \mathbf{h}_{\text{pert}}^{(i)} = \varphi_{\text{rec}}(\mathbf{s}^{(i)}). \quad (1)$$

In parallel, we extract local k -gram representations from each sequence:

$$\begin{aligned} \mathbf{p}_{\text{orig}} &= \{\varphi_{\text{rec}}(\mathbf{s}[t:t+k])\}_{t=1}^{L-k}, \\ \mathbf{p}_{\text{pert}}^{(i)} &= \left\{ \varphi_{\text{rec}}(\mathbf{s}^{(i)}[t:t+k]) \right\}_{t=1}^{L-k}. \end{aligned} \quad (2)$$

We define the sample-feature spaces as $\mathbb{X}_{\text{orig}} = (\mathbf{h}_{\text{orig}}, \mathbf{p}_{\text{orig}}, \xi_{\text{orig}})$ and $\mathbb{X}_{\text{pert}}^{(i)} = (\mathbf{h}_{\text{pert}}^{(i)}, \mathbf{p}_{\text{pert}}^{(i)}, \xi_{\text{pert}})$, where ξ is a scalar interaction function, e.g., dot-product or neural similarity). Following the UCOOT formulation (Tran et al. 2023), the DLOT distance is defined as:

$$\text{DLOT}_{\lambda}(\mathbb{X}_{\text{orig}}, \mathbb{X}_{\text{pert}}^{(i)}) = \min_{\pi^s, \pi^f} \left[\iint |\xi_{\text{orig}}(h_i, p_k) - \xi_{\text{pert}}(h_j, p_l)|^p d\pi^s(i, j) d\pi^f(k, l) + \sum_{j=1}^2 \lambda_j \text{KL}(\pi_{\#j}^s \otimes \pi_{\#j}^f \| \mu_j^s \otimes \mu_j^f) \right],$$

which subjects to the constraint $m(\pi^s) = m(\pi^f)$. This objective captures both global and local alignment under unbalanced settings, where marginal relaxation enables robustness to noise or perturbations.

The corresponding reward is defined as the negative DLOT value:

$$R_{\text{dist}}^{(i)} = -\text{DLOT}_{\lambda}(\mathbb{X}_{\text{orig}}, \mathbb{X}_{\text{pert}}^{(i)}), \quad (3)$$

which encourages perturbed sequences to remain distributionally consistent with the original in both global and compositional representations.

Optimization via BCD and Sinkhorn Algorithm

To solve the DLOT objective efficiently, we adopt the *Block Coordinate Descent (BCD)* algorithm proposed for (Tran et al. 2023), with alternating updates for the sample-level transport plan π^s and feature-level plan π^f .

Sinkhorn Update Each transport plan update in Algorithm 1 solves an unbalanced optimal transport problem with KL divergence regularization. The generic form is:

$$\min_{\pi \in \mathbb{R}_+^{n \times m}} \langle C, \pi \rangle + \lambda \text{KL}(\pi \| r \otimes c) + \varepsilon \text{KL}(\pi \| \mathbf{1}), \quad (4)$$

Algorithm 1: BCD Algorithm to Solve DLOT via UCOOT

Require: Representations $(\mathbf{h}_{\text{orig}}, \mathbf{p}_{\text{orig}})$, $(\mathbf{h}_{\text{pert}}, \mathbf{p}_{\text{pert}})$, interactions $\xi_{\text{orig}}, \xi_{\text{pert}}$, weights λ_1, λ_2 , entropic regularization ε , iterations T

Ensure: The final transport plans π^s, π^f

- 1: Initialize π^s, π^f
 - 2: **for** $t = 1, \dots, T$ **do**
 - 3: Compute cost matrix C^s using current π^f
 - 4: Update π^s via entropic Sinkhorn (see below)
 - 5: Rescale $\pi^s \leftarrow \sqrt{m(\pi^f)/m(\pi^s)} \cdot \pi^s$
 - 6: Compute cost matrix C^f using updated π^s
 - 7: Update π^f via entropic Sinkhorn
 - 8: Rescale $\pi^f \leftarrow \sqrt{m(\pi^s)/m(\pi^f)} \cdot \pi^f$
 - 9: **end for**
-

where $C \in \mathbb{R}^{n \times m}$ is the cost matrix, $r \in \Delta^n$, $c \in \Delta^m$ are relaxed (non-normalized) marginal histograms (e.g., uniform), λ controls the divergence penalty (mass conservation), ε is the entropic regularization weight.

The solution is obtained via multiplicative Sinkhorn iterations. Define the Gibbs kernel $K = \exp(-C/\varepsilon)$. The update proceeds is that we first initialize $u \leftarrow \mathbf{1}_n$ and $v \leftarrow \mathbf{1}_m$, then we repeat for T_{inner} iterations or until convergence:

$$u \leftarrow \left(\frac{r}{Kv} \right)^{\lambda/(\lambda+\varepsilon)}, \quad (5)$$

$$v \leftarrow \left(\frac{c}{K^T u} \right)^{\lambda/(\lambda+\varepsilon)}. \quad (6)$$

Finally, the transport plan is reconstructed as:

$$\pi = \text{diag}(u) \cdot K \cdot \text{diag}(v). \quad (7)$$

This iterative scheme solves the optimality conditions of Eq. (4). The exponent $\lambda/(\lambda + \varepsilon)$ balances mass fidelity and entropy.

Numerical Stabilization To prevent underflow when ε is small or C has large entries, it is common to perform the iterations in the log-domain:

$$\log u \leftarrow \frac{\lambda}{\lambda + \varepsilon} (\log r - \log(Kv)), \quad (8)$$

$$\log v \leftarrow \frac{\lambda}{\lambda + \varepsilon} (\log c - \log(K^T u)).$$

Cost Matrix Computation In our DLOT context, the cost matrices C^s and C^f are recomputed at each BCD iteration using the other coupling:

$$C_{ij}^s = \sum_{k,l} |\xi_{\text{orig}}(h_i, p_k) - \xi_{\text{pert}}(h_j, p_l)|^p \cdot \pi_{kl}^f, \quad (9)$$

$$C_{kl}^f = \sum_{i,j} |\xi_{\text{orig}}(h_i, p_k) - \xi_{\text{pert}}(h_j, p_l)|^p \cdot \pi_{ij}^s. \quad (10)$$

These are weighted average discrepancies between sample-feature interactions across domains, used to guide alignment.

B Derivation of Constrained Reinforcement with Dynamic Barrier

To dynamically adjust the penalty coefficient δ in the Lagrangian $\mathcal{L}(\psi, \delta)$, we formulate a constrained optimization subproblem that balances reward maximization and constraint satisfaction. This derivation extends the bi-level optimization framework to reinforcement learning with policy gradients. Below, we provide a step-by-step expansion of the mathematical reasoning.

Constrained Optimization Reformulation

The primal optimization problem aims to maximize the combined rewards \mathcal{J}_{dir} and \mathcal{J}_{div} while ensuring the stealth constraint $\mathcal{J}_{\text{dist}} \leq \rho_{st}$ is satisfied. Formally:

$$\max_{\psi} \underbrace{\mathcal{J}_{\text{dir}}(\psi) + \mathcal{J}_{\text{div}}(\psi)}_{\text{Reward Objectives}} \quad \text{s.t.} \quad \underbrace{\mathcal{J}_{\text{dist}}(\psi) \leq \rho_{st}}_{\text{Stealth Constraint}}. \quad (11)$$

To handle the constraint, we employ Lagrangian relaxation, which converts the constrained problem into a saddle-point problem. The Lagrangian $\mathcal{L}(\psi, \delta)$ introduces a penalty coefficient $\delta \geq 0$ to penalize constraint violations:

$$\min_{\delta \geq 0} \max_{\psi} \mathcal{L}(\psi, \delta) = \mathcal{J}_{\text{dir}} + \mathcal{J}_{\text{div}} - \delta (\mathcal{J}_{\text{dist}} - \rho_{st}). \quad (12)$$

Here, δ acts as a dual variable that adaptively scales the penalty based on the degree of constraint violation $\mathcal{J}_{\text{dist}} - \rho_{st}$. The min-max formulation allows simultaneous optimization of the policy ψ (maximizing rewards) and the penalty δ (minimizing constraint violations).

Gradient Alignment Objective

A critical challenge arises when gradients of the reward objectives ($\nabla \mathcal{J}_{\text{dir}}, \nabla \mathcal{J}_{\text{div}}$) and constraint ($\nabla \mathcal{J}_{\text{dist}}$) conflict. To mitigate this, we design a secondary objective $\mathcal{J}(\delta)$ that enforces alignment between reward and constraint gradients. Specifically, $\mathcal{J}(\delta)$ minimizes the Euclidean distance between the combined reward gradient and the scaled constraint gradient, while also penalizing constraint violations:

$$\mathcal{J}(\delta) = \underbrace{\frac{1}{2} \|\nabla_{\psi}(\mathcal{J}_{\text{dir}} + \mathcal{J}_{\text{div}}) - \delta \nabla_{\psi} \mathcal{J}_{\text{dist}}\|^2}_{\text{Gradient Alignment}} - \underbrace{\delta (\mathcal{J}_{\text{dist}} - \rho_{st})}_{\text{Violation Penalty}}. \quad (13)$$

The first term ensures that the direction of policy updates (driven by rewards) does not contradict the constraint gradient. The second term directly penalizes deviations from the stealth bound ρ_{st} .

Solve for Optimal δ

To find the optimal δ , we take the derivative of $\mathcal{J}(\delta)$ with respect to δ and set it to zero:

$$\frac{\partial \mathcal{J}}{\partial \delta} = (\nabla_{\psi} \mathcal{J}_{\text{dist}})^{\top} (\nabla_{\psi}(\mathcal{J}_{\text{dir}} + \mathcal{J}_{\text{div}}) - \delta \nabla_{\psi} \mathcal{J}_{\text{dist}}) - (\mathcal{J}_{\text{dist}} - \rho_{st}) = 0. \quad (14)$$

Rearranging terms yields a closed-form solution for δ :

$$\delta = \frac{\underbrace{(\mathcal{J}_{\text{dist}} - \rho_{st})}_{\text{Constraint Violation}} + \underbrace{\nabla_{\psi} \mathcal{J}_{\text{dist}}^{\top} \nabla_{\psi} (\mathcal{J}_{\text{dir}} + \mathcal{J}_{\text{div}})}_{\text{Gradient Conflict Term}}}{\underbrace{\|\nabla_{\psi} \mathcal{J}_{\text{dist}}\|^2}_{\text{Normalization by Constraint Gradient Magnitude}}}. \quad (15)$$

This expression reveals that δ increases when the constraint is violated ($\mathcal{J}_{\text{dist}} > \rho_{st}$) or when the reward and constraint gradients are aligned (positive inner product). Conversely, conflicting gradients reduce δ to prioritize reward maximization.

Policy Gradient Expansion

Using the policy gradient theorem, we express the gradients $\nabla_{\psi} \mathcal{J}_r$ ($r \in \{\text{dir}, \text{div}, \text{dist}\}$) as expectations over trajectories sampled from the policy π_{ψ} . For each reward or constraint term:

$$\nabla_{\psi} \mathcal{J}_r = \mathbb{E}_{\tau \sim \pi_{\psi}} \left[\sum_{t=0}^T \nabla_{\psi} \log \pi_{\psi}(a_t | s_t) \cdot A_{R_r}(s_t, a_t) \right], \quad (16)$$

where $A_{R_r}(s_t, a_t)$ denotes the advantage function for reward R_r , estimating how much better an action a_t is compared to the average at state s_t . Substituting these expectations into the expression for δ gives:

$$\delta = \frac{(\mathcal{J}_{\text{dist}} - \rho_{st})}{\|\mathbb{E}_{\tau} [\sum_t \nabla_{\psi} \log \pi_{\psi} \cdot A_{\mathcal{J}_{\text{dist}}}] \|^2} + \frac{\mathbb{E}_{\tau} [\sum_t \nabla_{\psi} \log \pi_{\psi} \cdot A_{\mathcal{J}_{\text{dist}}}]^{\top} \mathbb{E}_{\tau} [\sum_t \nabla_{\psi} \log \pi_{\psi} \cdot (A_{\mathcal{J}_{\text{dir}}} + A_{\mathcal{J}_{\text{div}}})]}{\|\mathbb{E}_{\tau} [\sum_t \nabla_{\psi} \log \pi_{\psi} \cdot A_{\mathcal{J}_{\text{dist}}}] \|^2}. \quad (17)$$

This formulation explicitly connects δ to the advantage-weighted policy gradients, ensuring updates account for both immediate and long-term effects of actions.

Dynamic Barrier Regularization

To ensure numerical stability and avoid division by zero, we add a small constant $\kappa > 0$ to the denominator. Additionally, we enforce non-negativity of δ through the operator $[\cdot]_+ = \max(\cdot, 0)$, which projects negative values to zero:

$$\delta = \left[\frac{\mathcal{J}_{\text{dist}} - \rho_{st} - \nabla_{\psi} \mathcal{J}_{\text{dist}}^{\top} \nabla_{\psi} (\mathcal{J}_{\text{dir}} + \mathcal{J}_{\text{div}})}{\|\nabla_{\psi} \mathcal{J}_{\text{dist}}\|^2 + \kappa} \right]_+. \quad (18)$$

The term $-\nabla_{\psi} \mathcal{J}_{\text{dist}}^{\top} \nabla_{\psi} (\mathcal{J}_{\text{dir}} + \mathcal{J}_{\text{div}})$ quantifies the conflict between reward and constraint gradients. If they oppose each other (negative inner product), δ decreases to prioritize reward maximization. Severe constraint violations ($\mathcal{J}_{\text{dist}} \gg \rho_{st}$) dominate the numerator, increasing δ to suppress detectable perturbations. The policy gradients are derived as:

$$\begin{aligned} \nabla_{\psi} (\mathcal{J}_{\text{dir}} + \mathcal{J}_{\text{div}}) &= \mathbb{E}_{\tau} \left[\sum_t \nabla_{\psi} \log \pi_{\psi}(a_t | s_t) \cdot (\hat{A}_{R_{\text{dir}}} + \hat{A}_{R_{\text{div}}}) \right], \\ \nabla_{\psi} \mathcal{J}_{\text{dist}} &= \mathbb{E}_{\tau} \left[\sum_t \nabla_{\psi} \log \pi_{\psi}(a_t | s_t) \cdot \hat{A}_{R_{\text{dist}}}(s_t, a_t) \right]. \end{aligned} \quad (19)$$

The term $\mathcal{J}_{\text{dist}} - \rho_{st}$ directly measures the severity of stealth constraint violation. The inner product term evaluates the alignment between constraint gradients ($\nabla \mathcal{J}_{\text{dist}}$) and combined reward gradients ($\nabla \mathcal{J}_{\text{dir}} + \nabla \mathcal{J}_{\text{div}}$). Negative alignment (conflict) reduces δ , allowing greater emphasis on rewards. Normalizes the penalty by the squared magnitude of constraint gradients, stabilizing updates across varying gradient scales. The constant κ prevents division by near-zero values, ensuring numerical robustness. When constraints are satisfied ($\mathcal{J}_{\text{dist}} \leq \rho_{st}$) and gradients align, δ remains small, prioritizing attack efficacy. Severe violations or aligned gradients increase δ , enforcing stealthiness without sacrificing convergence stability.

This derivation rigorously extends the bi-level optimization framework to policy gradient RL, enabling adaptive trade-offs between attack efficacy and stealth. In practice, expectations are approximated via Monte Carlo sampling over trajectories generated by the current policy π_ψ . The dynamic barrier mechanism ensures constraints are softly enforced throughout training, adapting to evolving policy and environmental dynamics.

C Algorithm Summary

The algorithm of our proposed model CREAT is outlined in a two-stage optimization process in Algorithm 2. From lines 1-12, we introduce the Localization Stage, which initializes the perturbation masker and processes each training sequence. This phase involves generating perturbation masks and constructing perturbed sequences step by step while calculating the pattern inversion rewards. The transition at each step is stored for later analysis. From Lines 13-27, we describe the Constrained Fine-tuning Stage, focusing on fine-tuning the model through reinforcement learning. Here, the policy is updated using a constrained gradient to ensure both attack intensity, i.e., maximizing pattern inversion, and stealthiness i.e., minimizing distribution shifts. Group-wise baselines are calculated, and dynamic barriers adjust the penalty term to ensure that perturbations remain stealthy yet effective. This dual-level optimization ultimately converges to a policy capable of performing subtle, high-impact profile pollution attacks against sequential recommendation.

D Datasets and Implementation Details

Dataset Details

We use three real-world recommendation datasets to evaluate the proposed methods, i.e. MovieLens-1M (ML-1M), MovieLens-20M (ML-20M), and Amazon Beauty. We employ 5-core versions of the datasets and preprocess them according to (Sun et al. 2019). The last two items in each sequence are reserved for validation and testing, with the rest assigned to training. The details of the pre-processed datasets are shown in Table 4.

Implementation Details

For fair comparison, we follow the implementation in previous work when implementing backbone SR models and all baselines. The backbone models are uniformly trained using

Datasets	#User	#Item	Avg.len	Sparsity
ML-1M	6,040	3,416	165	95.2%
Beauty	22,363	12,101	9	99.9%
ML-20M	138,493	18,345	144	99.2%

Table 4: Statistics on Datasets.

the Adam optimizer with a learning rate of 0.001, weight decay of 0.01, and a fixed batch size of 64. In the reinforcement learning training, the Adam optimizer is employed with a learning rate of 1e-5. For the group-relative policy optimization, the group size is set to 32, and the number of policy updates per round is 20. Following previous works (Yue et al. 2021, 2022), we set the maximum sequence length to 200 for the ML-1M and ML-20M datasets and 50 for the Beauty dataset. In the baseline experiments, the maximum number of replacements is set to 2 for ML-1M and ML-20M, and 1 for Beauty, with the proportion of manipulable sequence subsets controlled by the attacker fixed at 10%. To evaluate the effectiveness of targeted attacks, we focus on metrics tailored to a specific targeted item. Hit Rate (HR@K) measures if the target item appears in the top-K recommendations:

$$\text{HR@K} = \frac{\sum_{u \in \mathcal{U}} \mathbb{I}(\text{rank}_u^{\text{target}} \leq K)}{|\mathcal{U}|}, \quad (20)$$

where \mathbb{I} is an indicator function, \mathcal{U} is the user set, and $\text{rank}_u^{\text{target}}$ is the rank of the targeted item for user u . Normalized Discounted Cumulative Gain (NDCG@K) evaluates the ranking position of the target item:

$$\text{NDCG@K} = \frac{1}{|\mathcal{U}|} \sum_{u \in \mathcal{U}} \frac{\mathbb{I}(\text{rank}_u^{\text{target}} \leq K) \cdot \frac{1}{\log_2(\text{rank}_u^{\text{target}} + 1)}}{\text{IDCG@K}_u}. \quad (21)$$

Here, IDCG@K_u is the ideal DCG@K (computed if the target item were ranked first). Mean Reciprocal Rank (MRR) assesses the average reciprocal rank of the targeted item:

$$\text{MRR} = \frac{1}{|\mathcal{U}|} \sum_{u \in \mathcal{U}} \frac{1}{\text{rank}_u^{\text{target}}}. \quad (22)$$

We conduct our experiment on a Ubuntu OS with version 22.04.4 LTS, which contains 4 NVIDIA RTX 3090 GPUs, 2 64-bit 12-core Intel(R) Xeon(R) Silver 4116 CPUs @ 2.10GHz and 503GB of RAM.

E Attack Performance Under Defense

To evaluate the stealthiness of CREAT, we employ the defense method ADVTrain (Yue et al. 2022), which is specifically designed for profile pollution attacks. We utilize ADVTrain to defend against three attack SOTAs and our attack CREAT on two SR backbones. From the results in Table 5, we can conclude: 1) CREAT causes less disruption of attack performance than other attacks (measured by relative degradation: $\frac{P_{\text{undef}} - P_{\text{def}}}{P_{\text{undef}}}$, where P_{undef} and P_{def} represent attack performance on undefended and defended models, respectively), indicating the superiority of CREAT in evading

the ADVTrain defense. This further validates the efficacy of the constraint reward on the perturbed sequence distribution in CREAT, which minimizes the perturbation magnitude while achieving similar attack effectiveness, thereby weakening the defense method’s ability to detect and counter the perturbed sequences. 2) CREAT achieves powerful attack performance on both backbones with or without defending, demonstrating its robustness across different scenarios.

Attack	NARM		Bert4Rec	
	H@10	N@10	H@10	N@10
SimAlter	0.0257(↓51.14%)	0.0103(↓51.42%)	0.0201(↓55.73%)	0.0099(↓48.97%)
Replace	0.0464(↓38.95%)	0.0177(↓44.39%)	0.0309(↓51.49%)	0.0163(↓52.19%)
SSLAttack	0.0417(↓44.69%)	0.0165(↓48.02%)	0.0383(↓44.81%)	0.0201(↓45.97%)
CREAT	0.0825(↓27.12%)	0.0379(↓30.84%)	0.0787(↓26.45%)	0.0351(↓29.52%)

Table 5: Attack performance under defenses.

F Discussion on Potential Positive and Negative Societal Impacts

The proposed CREAT framework for profile pollution attacks against sequential recommendation systems presents several potential societal impacts that warrant careful consideration. On the positive side, this work contributes to the broader understanding of adversarial vulnerabilities in recommendation systems, a critical step toward building more secure and trustworthy AI systems. By exposing the risks of stealthy perturbations targeting fine-grained sequential patterns, this research motivates the development of robust defense mechanisms, ultimately enhancing the resilience of recommendation algorithms against malicious manipulation. Furthermore, the bi-level optimization framework and constrained reinforcement learning paradigm introduced in CREAT may inspire novel methodologies for adversarial robustness research beyond recommendation systems, such as in fraud detection or anomaly identification, where balancing efficacy and stealthiness is paramount. Conversely, the attack methodology itself could be misused by malicious actors to artificially inflate the visibility of specific items (e.g., misinformation, counterfeit products, or biased content) while evading detection, undermining user trust and platform integrity. To mitigate such risks, the authors explicitly emphasize the necessity of future work on adaptive defense strategies and advocate for responsible disclosure through controlled code release. By proactively addressing these dual-use implications, this work aligns with ethical AI research practices, advancing security knowledge while highlighting the urgency of safeguarding recommendation ecosystems.

Algorithm 2: The proposed framework CREAT

Require: Sequential recommender Φ_θ , Training sequences $\mathcal{S} \subseteq \mathcal{D}$, Target item v^* , Perturbation budget K

Ensure: Optimized perturbation masker \mathcal{M}_ψ

- 1: Initialize perturbation masker \mathcal{M}_ψ with parameters ψ
- 2: Initialize group-shared experience replay buffer \mathcal{B}
- 3: *Stage 1: The Localization Stage*
- 4: **for** each sequence $\mathbf{s} \in \mathcal{S}$ **do**
- 5: $\mathbf{s}'^{(0)} \leftarrow \mathbf{s}, T^{(0)} \leftarrow \emptyset$
- 6: **for** step $i = 1$ to K **do**
- 7: Generate mask $\mathbf{m}^{(i)} \sim \mathcal{M}_\psi(\mathbf{s}'^{(i-1)})$
- 8: Construct perturbed sequence:
- 9: $\mathbf{s}'^{(i)} \leftarrow \mathbf{s}'^{(i-1)} \odot (1 - \mathbf{m}^{(i)}) + v^* \cdot \mathbf{m}^{(i)}$
- 10: $T^{(i)} \leftarrow T^{(i-1)} \cup \{t_j | \mathbf{m}_t^{(i)} = 1\}$
- 11: Compute pattern inversion reward:
- 12: $R_{\text{inv}}^{(i)} = R_{\text{dir}}^{(i)} + R_{\text{div}}^{(i)}$
- 13: Store transition $(\mathbf{s}'^{(i-1)}, \mathbf{m}^{(i)}, R_{\text{inv}}^{(i)}, \mathbf{s}'^{(i)})$ in \mathcal{B}
- 14: **end for**
- 15: **end for**
- 16: Update ψ via policy gradient: $\psi \leftarrow \psi + \eta \nabla_\psi \mathcal{J}_{\text{inv}}$
- 17: *Stage 2: The Constrained Stage*
- 18: **while** not converged **do**
- 19: Sample group of G trajectories from \mathcal{B}
- 20: **for** each trajectory $(\mathbf{s}'^{(0)}, \dots, \mathbf{s}'^{(K)})$ **do**
- 21: **for** each step i **do**
- 22: Compute distribution consistency reward:
- 23: $R_{\text{dist}}^{(i)} = -\text{DLOT}(\mathbb{X}_{\text{orig}}, \mathbb{X}_{\text{pert}}^{(i)})$
- 24: **end for**
- 25: **end for**
- 26: Compute group-wise baseline μ_G and σ_G
- 27: Set dynamic stealth threshold:
- 28: $\rho_{st} = \mu_G^{\text{dist}} + \lambda_{st} \cdot \sigma_G^{\text{dist}}$
- 29: Calculate dynamic barrier coefficient:
- 30: $\delta = \left[\frac{\mathcal{J}_{\text{dist}} - \rho_{st} - \nabla_\psi \mathcal{J}_{\text{dist}}^\top \nabla_\psi (\mathcal{J}_{\text{dir}} + \mathcal{J}_{\text{div}})}{\|\nabla_\psi \mathcal{J}_{\text{dist}}\|^2 + \kappa} \right]_+$
- 31: Compute normalized advantage estimates:
- 32: $\hat{A}_{i,t} = \frac{r_{i,t} - \mu_{G,t}}{\sigma_{G,t} + \epsilon}$
- 33: Update policy with constrained gradient:
- 34: $\nabla_\psi \mathcal{L} = \nabla_\psi \mathcal{J}_{\text{dir}} + \nabla_\psi \mathcal{J}_{\text{div}} - \delta \cdot \nabla_\psi \mathcal{J}_{\text{dist}}$
- 35: $\psi \leftarrow \psi + \eta \nabla_\psi \mathcal{L}$
- 36: **end while**
